Ab initio molecular dynamics with an orthonormalized mixed basis

1995 J. Phys.: Condens. Matter 7 6197

(http://iopscience.iop.org/0953-8984/7/31/004)

J. Phys.: Condens. Matter 7 (1995) 6197–6209. Printed in the UK

Ab initio molecular dynamics with an orthonormalized mixed basis

Tatsuya Kishi and Satoshi Itoh

Advanced Research Laboratory, Toshiba Corporation, 1 Komukai Toshiba-cho, Saiwai-ku, Kawasaki 210, Japan

Received 21 March 1995, in final form 26 May 1995

Abstract. We present a formulation of *ab initio* molecular dynamics with a mixed basis. The mixed basis is constructed by a plane-wave set and localized basis functions which are defined by spatially localized functions. The basis functions are orthonormalized with each other, and the equations of motion for wavefunctions of electrons are simplified. Forces acting on atoms include the Pulay terms, which are explicitly represented in the present formulation. This method is tested on diamond and applied iron as a first step in studying the effect of spin polarization.

1. Introduction

Ab initio molecular dynamics proposed by Car and Parrinello [1] is a powerful method which unifies the calculation of the electronic states and the molecular dynamics, and is now widely applied for semiconductors or simple metals. The use of pseudopotentials with a plane-wave basis set plays an important role in the calculations for these materials by means of this method. Plane-wave expansion can work well when the pseudopotentials are used simultaneously, because the pseudopotentials are much weaker than the real Coulomb potentials, especially for most semiconductors and the simple metals. For first-row elements and transition metals, however, this method must be applied with some care, because these elements have strong pseudopotentials [2]. One way to calculate the electronic properties efficiently for these elements is to use relatively soft pseudopotentials. Calculations with an ultrasoft pseudopotential [3] have been reported for molecular oxygen [4] and liquid copper [5]. Another method of calculation is to use a localized basis set and norm-conserving pseudopotentials. We employ here the latter, in particular a *mixed-basis approach*.

A mixed-basis approach, which combines plane waves and localized functions in the basis set, is introduced to efficiently treat the atomic-like wavefunctions in solids [6–8]. In [6] the Bloch sums of the Gaussian orbitals are used as the localized part of the basis set. This is the reason why the Hamiltonian and the overlap matrix can be analytically expressed using the Fourier transform of the Gaussian orbitals which have the analytic representation of the Fourier transform. However, this choice of the localized part of the basis set leads to solving of generalized matrix eigenvalue problem, which includes the Hamiltonian matrix and the overlap matrix of the basis.

While a mixed-basis formalism is appropriate for calculation of the materials incorporating localized d electrons, it is more complicated and requires increasing calculation time. In order to overcome this difficulty, there is a way to construct an *orthonormalized* basis set from a mixed-basis set. This was proposed by Jansen, Sankey and Klein (JSK) [9] several years ago. JSK constructed an orthonormalized mixed-basis set from plane waves

0953-8984/95/316197+13$19.50

and pseudoatomic orbitals (PAO) to represent the wavefunctions that have atomic-orbital features. It is noted that PAO employed by JSK are computed self-consistently for the pseudopotentials of a free atom. Rappe and co-workers [10] have pointed out that the JSK mixed-basis set is not overcomplete and takes advantage of iterative minimization schemes for electronic and atomic degrees of freedom.

We note here that the localized functions, which are the origin of the localized part of a mixed-basis set, are only used as constituents constructing a basis. In principle, one can choose *any* functions to constitute a basis. Using this property of the mixed basis, we present a novel mixed-basis approach which is suitable for an *ab initio* molecular dynamics calculation. The key idea of our orthonormalized mixed-basis approach is to make use of a momentum-space representation for localized functions. This approach leads to a simpler formulation and more efficient calculation for the electronic states of the system if the localized function contains an analytic expression of the Fourier transform. In addition, we can explicitly represent the Pulay term of the force acting on atoms.

We applied the mixed-basis approach for *ab initio* molecular dynamics to diamond as a first-row material, because the properties of diamond were studied by experimental and theoretical methods [11, 12] many years ago. This method was also applied to iron, as a transition metal, which may be the first trial using this approach for studying materials with non-zero spin polarization.

This paper is organized as follows. In section 2 we describe the construction of the mixed basis. In section 3 we present the formulation for *ab initio* molecular dynamics with the mixed-basis set described in the previous section. In section 4 the force formula, especially the *Pulay term*, are given. In section 5 we calculate the electronic structure and the lattice dynamics of diamond and iron. Finally, in section 6 we summarize our results.

2. Mixed basis

A mixed-basis set is introduced [6] to express effectively the wavefunctions of the electrons in a crystal that have localized features. The mixed-basis set consists of a localized part and a delocalized (plane-wave-like) part, and is suitable for representing both localized states and extended states of the system. However, a mixed-basis set is overcomplete and not orthonormal, in general. For this reason, calculations based on a mixed basis are more complex and require a great deal of computer time. To avoid this difficulty, we introduce an *orthonormalized* mixed basis which is constructed from plane waves and a localized basis. We expand the wavefunction of the electron with band index j, wave vector $\boldsymbol{k}$ and spin σ as follows:

$$\psi^{\sigma}_{j\boldsymbol{k}}(\boldsymbol{r}) = \frac{1}{\sqrt{\Omega}} \sum_{\boldsymbol{G}_1} c^{\sigma}_{j}(\boldsymbol{k}+\boldsymbol{G}_1) \mathrm{e}^{\mathrm{i}(\boldsymbol{k}+\boldsymbol{G}_1)\cdot\boldsymbol{r}} + \sum_{s,\mu} d^{\sigma}_{j\boldsymbol{k}s\mu} \varphi_{\boldsymbol{k}s\mu}(\boldsymbol{r}) \tag{1}$$

where Ω is the volume of the unit cell and $\boldsymbol{G}_1$ is the reciprocal lattice vector. The symbol s, μ means that the μth basis function is connected to the sth atom in the unit cell. The orthonormality conditions of the basis set are represented by

$$\begin{aligned} &\langle \boldsymbol{k}+\boldsymbol{G}|\boldsymbol{k}+\boldsymbol{G}'\rangle = \delta_{\boldsymbol{G},\boldsymbol{G}'} \\ &\langle \boldsymbol{k}+\boldsymbol{G}|\boldsymbol{k}'s'\mu'\rangle = 0 \\ &\langle \boldsymbol{k}s\mu|\boldsymbol{k}'s'\mu'\rangle = \delta_{\boldsymbol{k}\boldsymbol{k}'}\delta_{ss'}\delta_{\mu\mu'} \end{aligned} \tag{2}$$

where

$$\langle r|k+G\rangle = \frac{1}{\sqrt{\Omega}} e^{i(k+G)\cdot r} \tag{3}$$

and

$$\langle r|ks\mu\rangle = \varphi_{ks\mu}(r) \tag{4}$$

which is the localized part of the mixed-basis set.

The mixed-basis set in the present approach is constructed as follows. In the first step, we choose spatially localized functions f_μ ($\mu = 1, \ldots, m$) and generate the Bloch function for each k vector in the reduced Brillouin zone:

$$\phi_{ks\mu}(r) = \frac{1}{\sqrt{\Omega}} \sum_{\tau R_s} e^{ik\cdot(\tau+R_s)} f_{s\mu}(r-\tau-R_s) \tag{5}$$

where τ is the Bravais-lattice vector and R_s is the position vector of the sth atom in the unit cell. The symbol $f_{s\mu}$ means the localized function f_μ is linked to the sth atom. In the second step, we orthogonalize the function, $\phi_{ks\mu}$, to all plane waves with energy less than or equal to a cut-off energy, G_{pw}. This can be easily done by using the Fourier expansions of the Bloch functions defined above. Introducing a cut-off energy G_{max} ($\geqslant G_{pw}$) for the Fourier expansions of the Bloch functions, the function orthogonalized to the plane waves is given by

$$\phi_{ks\mu}(r) = \sum_{G_{pw}<G_2<G_{max}} \tilde{\phi}_{s\mu}(k+G_2) e^{i(k+G_2)\cdot r}. \tag{6}$$

The Fourier coefficients $\tilde{\phi}_{s\mu}(k+G_2)$ are

$$\tilde{\phi}_{s\mu}(k+G_2) = \frac{1}{\Omega} \tilde{f}_{s\mu}(k+G_2) e^{-iG_2\cdot R_s} \tag{7}$$

where $\tilde{f}_{s\mu}(k+G)$ is the Fourier coefficient of the localized function:

$$\tilde{f}_{s\mu}(k+G) = \frac{1}{\Omega} \int dr\ e^{-i(k+G)\cdot r} f_{s\mu}(r). \tag{8}$$

In the third step, the functions (6) are orthonormalized with each other by diagonalizing the overlap matrix. The overlap matrix $S_{s\mu;s'\mu'}$ is defined as

$$S_{s\mu;s'\mu'} = \langle \phi_{ks\mu} \mid \phi_{ks'\mu'} \rangle. \tag{9}$$

The unitary matrix U, which diagonalizes the overlap matrix, is obtained by solving the eigenvalue problem for the overlap matrix

$$USU^\dagger = D \tag{10}$$

where D is the diagonal matrix whose elements are given by

$$D_{s\mu;s'\mu'} \equiv \lambda_{s\mu}\delta_{s\mu;s'\mu'} \tag{11}$$

and $\lambda_{s\mu}$ is the eigenvalue of the matrix S. Note that the size of the overlap matrix S is Mm, where M is the number of atoms in the unit cell. This size of S is so small that there is practically no additional time for the calculation of the diagonalization of S. We also see that the diagonalization does not take so much time when treating a larger system, since the size of S depends linearly on M, not on the number of bands. Then the localized part of the orthogonalized basis set is generated by

$$\varphi_{ks\mu}(\boldsymbol{r}) = \frac{1}{\sqrt{\lambda_{s\mu}}} \sum_{s'\mu'} U_{s'\mu';s\mu}\phi_{ks'\mu'} = \sum_{G_{pw}<G_2<G_{max}} \tilde{\varphi}_{s\mu}(\boldsymbol{k}+\boldsymbol{G}_2)\mathrm{e}^{\mathrm{i}(\boldsymbol{k}+\boldsymbol{G}_2)\cdot\boldsymbol{r}} \tag{12}$$

where

$$\tilde{\varphi}_{s\mu}(\boldsymbol{k}+\boldsymbol{G}_2) = \frac{1}{\sqrt{\lambda_{s\mu}}} \sum_{s'\mu'} U_{s'\mu';s\mu}\tilde{f}_{s'\mu'}(\boldsymbol{k}+\boldsymbol{G}_2)\mathrm{e}^{-\mathrm{i}\boldsymbol{G}_2\cdot\boldsymbol{R}_{s'}}. \tag{13}$$

We note that there are no restrictions on choosing localized functions. While JSK have taken pseudoatomic orbitals as localized functions, we consider weighted Gaussian functions here [6]. The reason is that the Fourier transforms of these functions possess analytic representations and this is also expected to decrease the error in the calculation. The Gaussian-type orbital

$$r^l \exp(-\lambda r^2)Y_{lm}(\hat{\boldsymbol{r}}) \tag{14}$$

has the Fourier coefficients

$$\frac{1}{\Omega}\pi^{3/2}\lambda^{-l-3/2}(-\mathrm{i}G/2)^l \exp(-G^2/4\lambda)Y_{lm}(\hat{\boldsymbol{G}}) \tag{15}$$

where Y_{lm} are spherical harmonics.

3. Mixed-basis approach in *ab initio* molecular dynamics

Ab initio molecular dynamics introduced by Car and Parrinello [1] unifies an electronic-states calculation based on density functional theory and molecular dynamics. In density functional theory, the charge density which minimizes the total energy of the system is the exact ground-state density and the wavefunctions of the system are given by the self-consistent solution of the Kohn–Sham equations (for a review, see [13]). In the *ab initio* molecular dynamics approach, a fictitious time for wavefunctions of electrons is introduced and the system evolves obeying a fictitious dynamics. This dynamics is defined by a Lagrangian whose potential energy is given by the total energy of the system in density functional theory. The total energy per unit cell [14] is given by

$$E_{tot} = \sum_{j,\sigma} \int \mathrm{d}\boldsymbol{k}\, w_j^\sigma \epsilon_{jk}^\sigma u - E_H + M\bar{Z}_{val}\alpha_1 + \Delta E_{xc} + \gamma_E \tag{16}$$

where ϵ_{jk}^σ is the Kohn–Sham eigenvalue, w_j^σ is the occupation number of the jth band with spin σ

$$E_H = \frac{1}{2}\int \mathrm{d}\boldsymbol{r}\, V_H\rho \tag{17}$$

$$\alpha_1 = \frac{1}{\Omega_a}\int \mathrm{d}\boldsymbol{r}\left(V_{ps}^L(r) + \frac{2\bar{Z}_{val}}{r}\right) \tag{18}$$

$$\Delta E_{xc} = \int \mathrm{d}\boldsymbol{r}(\epsilon_{xc} - V_{xc})\rho \tag{19}$$

and

$$\gamma_E = \sum_{\tau,s,s'} \frac{z_s z_{s'}}{|\tau + R_s - R_{s'}|} - \frac{M(\bar{Z}_{val})^2}{\Omega_a} \int \mathrm{d}r \frac{1}{r}. \tag{20}$$

The density of the electron ρ is given by

$$\rho(r) = \sum_{j,\sigma} \int \mathrm{d}k \, w_j^\sigma |\psi_{jk}^\sigma(r)|^2. \tag{21}$$

The expressions $\bar{Z}_{val}$ and Ω_a mean

$$\bar{Z}_{val} = \frac{1}{M} \sum_{\text{unit cell}} z_s \tag{22}$$

and

$$\Omega_a = \frac{\Omega}{M} \tag{23}$$

respectively.

In the orthogonalized mixed-basis approach, the total energy of the system can be represented by the coefficients $c_j^\sigma(k+G)$ and $d_{jks\mu}^\sigma$ of the expansion of the wavefunction (1). We can express the Kohn–Sham eigenvalues which appear in the equation (16) as

$$\begin{aligned}\epsilon_{jk}^\sigma = & \sum_{G_1,G_1'} c_j^\sigma(k+G_1)^* \langle k+G_1|\mathcal{H}|k+G_1'\rangle c_j^\sigma(k+G_1') \\ & + \sum_{G_1,s\mu} c_j^\sigma(k+G_1)^* \langle k+G_1|\mathcal{H}|ks\mu\rangle d_{jks\mu}^\sigma + \text{CC} \\ & + \sum_{s\mu s'\mu'} d_{jks\mu}^{\sigma\,*} \langle ks\mu|\mathcal{H}|ks\mu\rangle d_{jks'\mu'}^\sigma \end{aligned} \tag{24}$$

where CC means the complex conjugate of the second term of (24). The symbol $\mathcal{H}$ is the Hamiltonian of the system defined by

$$\mathcal{H} = \frac{\delta E_{tot}}{\delta \rho}. \tag{25}$$

The sums of the first and second terms in (24) run over the reciprocal lattice vector G_1 or G_1', the absolute value of which is less than G_{pw}.

The Car–Parrinello Lagrangian which defines the fictitious dynamics is represented in the form

$$\begin{aligned}\mathcal{L} = & \sum_{i,\sigma} \int \mathrm{d}r \, \mathrm{d}k \; w_i^\sigma \frac{\mu_e}{2} |\dot{\psi}_{ik}^\sigma(r)|^2 + \sum_s \frac{M_s}{2} |\dot{R}_s|^2 - E_{tot}\left[\{\psi_{ik}^\sigma(r)\}, \{R_s\}\right] \\ & - \sum_{i,j,\sigma} \int \mathrm{d}k \, \Lambda_{ij}^{k\sigma} \left(\int \mathrm{d}r \psi_{ik}^\sigma(r)^* \psi_{jk}^\sigma(r) - \delta_{ij} \right) \end{aligned} \tag{26}$$

where μ_e is the fictitious mass of the electron, M_s is the mass of the sth atom and the third term is given by equation (16). The last term in equation (26) is introduced to conserve the orthonormality between the wavefunctions and Λ_{ij} is the corresponding Lagrange multiplier.

The equations of motion of the wavefunctions are derived from the Car–Parrinello Lagrangian (26). The minimization of the total energy is achieved by the time evolution determined by these equations as the system is gradually cooled. Here we employ a different approach to minimize the total energy of the system, that is, the direct minimization of the total energy by the steepest-descent method, which can be formulated in terms of first-order differential equations in the fictitious time as

$$\dot{\psi}^{\sigma}_{ik}(r) = -\frac{\delta E_{tot}}{\delta \dot{\psi}^{\sigma}_{ik}(r)^*}. \tag{27}$$

The equations for the expansion coefficients c^{σ}_{ik} and $d^{\sigma}_{iks\mu}$ of the wavefunction are given by

$$\mu_e \dot{c}^{\sigma}_j(k+G_1,t) = -\sum_{G_1'}\langle k+G_1|\mathcal{H}|k+G_1'\rangle c^{\sigma}_j(k+G_1',t) - \sum_{s\mu}\langle k+G_1|\mathcal{H}|ks\mu\rangle d^{\sigma}_{jks\mu}(t) + \sum_l \Lambda^{k\sigma}_{jl} c^{\sigma}_l(k+G_1,t) \tag{28}$$

and

$$\mu_e \dot{d}^{\sigma}_{jks\mu}(t) = -\sum_{G_1'}\langle ks\mu|\mathcal{H}|k+G_1'\rangle c^{\sigma}_j(k+G_1',t) - \sum_{s'\mu'}\langle ks\mu|\mathcal{H}|ks'\mu'\rangle d^{\sigma}_{jks'\mu'}(t) + \sum_l \Lambda^{k\sigma}_{jl} d^{\sigma}_{lks\mu}(t). \tag{29}$$

We note that the derivatives of the coefficients c^{σ}_{ik} and $d^{\sigma}_{iks\mu}$ are not included simultaneously in each equation of motion because of the orthonormality of the basis. Therefore we can easily treat these equations.

The equations of motion for atoms in the system are also derived from the Car–Parrinello Lagrangian. These are the second-order differential equations

$$M_s \ddot{R}_s = -\frac{\partial E_{tot}}{\partial R_s}. \tag{30}$$

We solve these equations to study the motions of atoms.

To calculate the matrix elements of the Hamiltonian which appear in equations (24), (28) and (29), we remember the localized part of the basis set is constructed in the form of Fourier expansions. Using equations (12) and (13), all matrix elements can be represented in the reciprocal space. The complete expressions of the matrix elements of the Hamiltonian are obtained as follows:

$$\langle k+G_1|\mathcal{H}|k+G_1'\rangle = |k+G_1|^2\delta_{G_1,G_1'} + V_L(G_1'-G_1) + V_{NL}(k+G_1,k+G_1') \tag{31}$$

$$\langle k+G_1|\mathcal{H}|ks\mu\rangle = \sum_{G_2} V_L(G_2-G_1)\tilde{\varphi}_{s\mu}(k+G_2) + \sum_{G_2} V_{NL}(k+G_1,k+G_2)\tilde{\varphi}_{s\mu}(k+G_2) \tag{32}$$

and

$$\langle ks\mu|\mathcal{H}|k's'\mu'\rangle = \sum_{G_2}|k+G_2|^2\tilde{\varphi}_{s\mu}(k+G_2)^*\tilde{\varphi}_{s'\mu'}(k+G_2) + \sum_{G_2,G_2'} V_L(G_2'-G_2)\tilde{\varphi}_{s\mu}(k+G_2)^*\tilde{\varphi}_{s'\mu'}(k+G_2') + \sum_{G_2,G_2'} V_{NL}(k+G_2,k+G_2')\tilde{\varphi}_{s\mu}(k+G_2)^*\tilde{\varphi}_{s'\mu'}(k+G_2'). \tag{33}$$

Here we use the representation of the Hamiltonian:

$$\mathcal{H} = -\nabla^2 + V_L + V_{NL} \tag{34}$$

where V_L and V_{NL} are the local and non-local parts of the potential, respectively. The local potential V_L consists of the Hartree potential, the exchange–correlation potential and the local part of the pseudopotential. The non-local potential is equal to the non-local part of the pseudopotential.

The use of the above expressions of the matrix elements has a great advantage in calculation. We need not evaluate the matrix elements of the potentials for the localized part of the mixed-basis set in the real space. Only the matrix elements of the potential in the reciprocal space with energy less than G_{max} are required. In practice, we can make good use of fast Fourier transforms (FFT) for evaluating the matrix elements. This leads to suppression of the increase in CPU time.

4. Hellmann–Feynman and Pulay forces

In the force calculation, we need to evaluate the Hellmann–Feynman force as well as the Pulay term due to the dependence of the basis functions on the positions of atoms. The force acting on atom s is given by

$$\boldsymbol{F}_s = -\frac{\partial E_{tot}}{\partial \boldsymbol{R}_s} = -\left\langle \Phi \left| \frac{\partial \mathcal{H}}{\partial \boldsymbol{R}_s} \right| \Phi \right\rangle - 2\mathrm{Re}\left(\left\langle \frac{\partial \Phi}{\partial \boldsymbol{R}_s} \middle| \mathcal{H} \middle| \Phi \right\rangle \right) \tag{35}$$

where $|\Phi\rangle$ denotes a state of the system, the first term of the right-hand side of this equation is the Hellmann–Feynman term and the second term is the Pulay term.

In the formulation which we adopt here, the Pulay term can be explicitly represented and then exactly calculated. By the definition of the force (35), and using the expression of the total energy (16), we obtain explicit representations of the force. The Hellmann–Feynman force is given by

$$\boldsymbol{F}_s^{HF} \equiv -\left\langle \Phi \left| \frac{\partial \mathcal{H}}{\partial \boldsymbol{R}_s} \right| \Phi \right\rangle = -\int \mathrm{d}\boldsymbol{r} \frac{\partial V_{ps}}{\partial \boldsymbol{R}_s} \rho. \tag{36}$$

To represent the Pulay term, we have to know the derivative of the wavefunction. Since the localized part of the basis set depends on the positions of atoms in the mixed-basis formalism, this term is not identical to zero. The derivative of the wavefunction is expressed as

$$\frac{\partial \psi_{jk}^{\sigma}(\boldsymbol{r})}{\partial \boldsymbol{R}_s} = \frac{1}{\Omega} \sum_{s'\mu' \boldsymbol{G}_2} d_{iks'\mu'}^{\sigma} \frac{\partial \tilde{\varphi}_{s\mu}(\boldsymbol{k}+\boldsymbol{G}_2)}{\partial \boldsymbol{R}_s} \mathrm{e}^{\mathrm{i}(\boldsymbol{k}+\boldsymbol{G}_2)\cdot\boldsymbol{r}} \tag{37}$$

using the Fourier expansions of the localized basis (12). The Fourier coefficients $\tilde{\varphi}_{s\mu}$ of the localized part of the basis set are given by equation (13). Note that the unitary transformation U, which appears in the Fourier coefficients (13), is defined for the fixed set of the position of atoms $\{\boldsymbol{R}_s\}$, and this includes $\{\boldsymbol{R}_s\}$ as parameters. Then we can explicitly represent the derivative of the coefficients as

$$\frac{\partial \psi_{jk}^{\sigma}(\boldsymbol{r})}{\partial \boldsymbol{R}_s} = \frac{1}{\Omega} \sum_{s'\mu' \boldsymbol{G}_2} (-\mathrm{i}\boldsymbol{G}_2) d_{iks'\mu'}^{\sigma} \left(\frac{1}{\sqrt{\lambda_{s'\mu'}}} \sum_{\mu''} \tilde{f}_{s\mu''}(\boldsymbol{k}+\boldsymbol{G}_2) U_{s\mu'';s'\mu'} \right) \mathrm{e}^{-\mathrm{i}\boldsymbol{G}_2\cdot\boldsymbol{R}_s}. \tag{38}$$

Substituting this equation into the second term of equation (35), we get the formula for the Pulay term of the force.

5. Applications

5.1. Electronic structure of diamond

In this section, we apply the method described above to carbon with diamond structure. Since the pseudopotential of carbon is deeper than that of silicon and there are many theoretical studies, it may be thought as an appropriate example for testing our mixed-basis approach.

For the mixed-basis calculation, we take a weighted Gaussian with spherical symmetry as a *spatially localized function*

$$f_{\mu=1}(r) = r^l \exp(-\lambda r^2). \tag{39}$$

Here we put $l = 2$ to represent the localized feature of the wavefunction effectively, though the carbon atom does not have orbitals with d symmetry. The Fourier coefficients of equation (39) is given by

$$\frac{1}{\Omega} N \pi^{2/3} (2\lambda)^{-5/2} \left(3 - \frac{G^2}{2\lambda}\right) e^{-G^2/4\lambda} \tag{40}$$

where N is the normalization constant

$$N = \left(\frac{4}{15} \frac{(2\lambda)^{7/2}}{\pi^{3/2}}\right)^{1/2}. \tag{41}$$

In the calculation we use the generalized norm-conserving pseudopotentials of Hamann [15], the Kleinman–Bylander form of the pseudopotential [15, 16], and the exchange–correlation potential of Perdew and Zunger [17]. We fix the cut-off energy as $G_{max} = 55.4$ Ryd, the fictitious mass for the wavefunction of the electron is set to $\mu_e = 300$ au, and the time step to $\Delta t = 10$ au. As a unit cell, a simple cubic supercell with a lattice constant $a = 3.57$ Å is taken and k-point summations are restricted to the Γ point. We stop iteration for minimization of the total energy with the fixed atoms if the convergence rate ϵ of the total energy is less than 1.0×10^{-5}. The convergence rate ϵ is defined by

$$\epsilon = \left| \frac{E(n) - E(n+1)}{E(n)} \right| \tag{42}$$

where $E(n)$ denotes the total energy of the system in the nth iteration.

Table 1. Cut-off energy dependence of the total energy. The cut-off energy G_{max} for the Fourier expansion is fixed as 55.4 Ryd.

G_{pw} (Ryd)	E_{tot} (Ryd/atom)
30.0	−10.94
40.0	−11.05
50.0	−11.09

In table 1 we show the dependence of the total energy per atom on the cut-off energy G_{pw} for the calculation based on the plane-wave basis. This indicates that the total energy almost converges for the cut-off energy $G_{pw} = 40\,\mathrm{Ryd}$, and we fix the cut-off energy as this value in the following calculation. We note that the cut-off energies G_{pw} and G_{max} correspond to 1357 and 2103 plane waves, respectively. This means that the computer memory required for the coefficients of the wavefunctions is smaller than that required for the plane-wave coefficients as a whole, because we have only to evolve the $1357 + 1$ coefficients. To determine the equilibrium lattice parameter for diamond, we calculate the total energy for four different lattice parameters and fit data with a parabolic curve. In figure 1 we show the total energy calculated and the fitting curve. The equilibrium lattice parameter is obtained as 3.72 Å and the experimental value is 3.57 Å. In the calculation below the lattice constant is fixed as the calculated equilibrium value. In figure 2 we display the fictitious time evolution of the total energy of the system for the cut-off energy of the plane wave $G_{pw} = 40\,\mathrm{Ryd}$ with the equilibrium lattice parameter determined above.

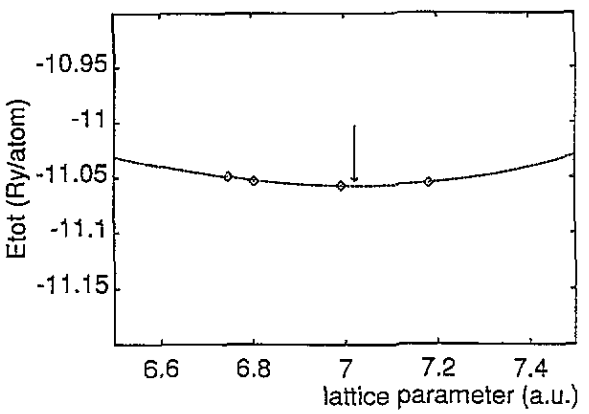

Figure 1. Calculated total energies against lattice parameters. We determine the equilibrium lattice parameter from a parabolic fitting to the total energies. The arrow indicates the equilibrium value of the lattice parameter.

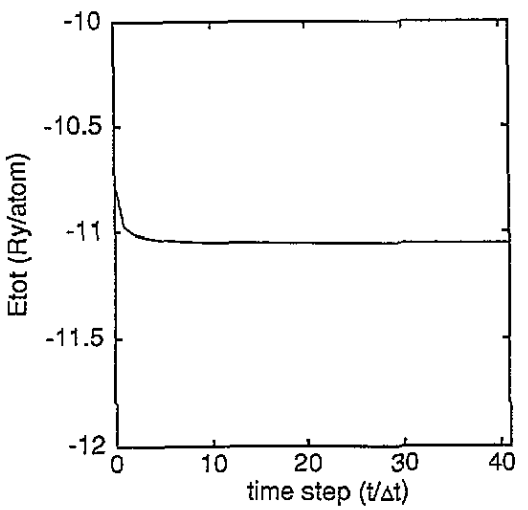

Figure 2. The time evolution of the total energy of the system. The cut-off energy for the plane-wave basis G_{pw} is 40 Ryd and the cut-off energy G_{max} is 55.4 Ryd. The total energy almost converges over ten iterations.

The Kohn–Sham eigenvalues are tabulated in table 2. The eigenvalues calculated by the plane-wave basis [11] with the Hamann–Schlüter–Chiang pseudopotential [2] and LAPW [12] are also tabulated for comparison. Since we use a simple cubic supercell in the calculation, the eigenvalues at the Γ point and the X point for the Brillouin zone of the face-centred cubic lattice appear at the Γ point of the Brillouin zone of the supercell. The degeneracies of the eigenvalues for the supercell from the lower-energy side are 1, 6, 6 and 3, respectively.

Table 2. Kohn–Sham eigenvalues. The eigenvalues calculated by plane-wave (17) basis with HSC pseudopotential and LAPW are also tabulated for comparison.

	This paper	PW	LAPW [12]
Γ_1	−22.21	−21.45	−21.36
$\Gamma_{25'}$	0	0	0
X_1	−13.28	−12.65	−12.61
X_4	−6.61	−6.22	−5.82

Next we study the lattice dynamics of diamond. We focus, in particular, on the optical phonon at the Γ point where the longitudinal and transverse modes are degenerate. The trajectories of the atoms are generated by solving the equation of motion (30). The initial displacement of each atom is determined for the velocities of atoms to give a Maxwell distribution at a fixed temperature and the temperature of the system is kept at 1000 K during the molecular dynamics calculation. In this calculation we omit the Pulay term for the non-local potential $-2\,\mathrm{Re}(\langle \partial\Phi/\partial R_s | V_{NL} | \Phi \rangle)$, because the Pulay term of the non-local potential is much smaller than that of the local potential. In figure 3, the motion of an atom along the ⟨111⟩ direction is depicted. This figure indicates that the optical mode has a frequency of 51.7 THz, which is comparable to the experimental value 39.96 THz [18].

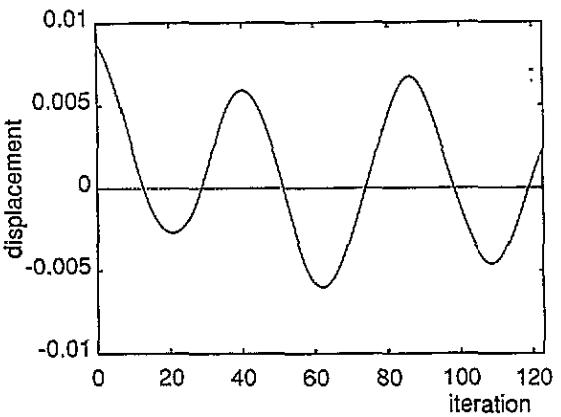

Figure 3. Motions of an atom of diamond with ⟨111⟩ mode. The frequency is about 20 iterations (one iteration corresponds to 4.8×10^{-16} s). The displacement has units of the lattice constant. The variation of the amplitude of the motion is influenced by the initial states for the atoms and disappears in the long-time limit.

5.2. Electronic structure of iron

The orthonormalized mixed-basis approach is applied to iron which has non-zero spin polarization. Since the pseudopotential of the iron atom is much stronger than most semiconductors, many basis functions are needed in the plane-wave basis approach. In

the orthonormalized mixed-basis approach many plane wavefunctions are also required, but the coefficients of the wavefunctions are far fewer than the number of plane waves. This reduces the amount of the computer memory and CPU time used in the calculations.

To calculate the electronic structure for iron, which has a body-centred cubic (bcc) structure, we use four special k points in the Brillouin zone summation, and fix the cut-off energy to $G_{max} = 300$ Ryd and $G_{pw} = 150$ Ryd, which correspond to 39 223 and 13 949 plane waves. Though we must evolve the $13\,149 + 1$ coefficients of the wavefunctions, this number is smaller than all 39 223 plane-wave coefficients. In this case we need only 1/3 of the computer memory for the coefficients in comparison with the plane-wave basis calculation, and this leads to less computational time used in the calculation. Iteration is stopped if the convergence rate ϵ of the total energy is less than 5.8×10^{-5}.

In order to determine the lattice constant we carry out the total energy calculation for the systems with the lattice constants 2.80 Å, 2.85 Å and 2.90 Å. Figure 4 shows the total energies as a function of the lattice parameter. The equilibrium lattice constant is determined from parabolic fitting and is 2.854 Å, as indicated by the arrow in the figure. This value is good agreement with the experimental value 2.866 Å. Unfortunately, the bulk modulus obtained from data is very much larger than the experimental value. It is supposed that the core correction for the pseudopotential is not taken into account here. The absence of the correction leads to an overestimation for the exchange–correlation energy. It has been indicated [19] that core corrections play an important role in the 3d transition metals obtaining their qualitative properties.

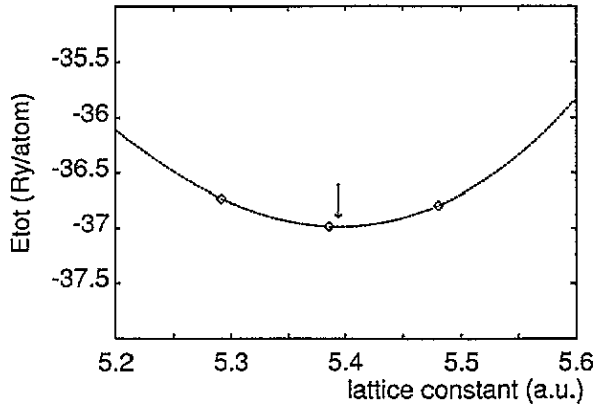

Figure 4. Calculated total energies for three lattice parameters and the parabolic fitting of these values. The arrow indicates the lattice constant that corresponds to the minimum of the total energy derived from the fitting curve.

The magnetic properties of iron as well as the electronic structures are interesting. The magnetic moment per atom converges more slowly than the total energy along the fictitious time evolution of the system. Continuing iteration to achieve the convergence rate fixed above for the total energy, we obtain 2.44 μ_B for the magnetic moment per atom with a lattice parameter 2.85 Å. It is found that the calculated value of the magnetic moment is slightly larger than the experimental value. This result comes from using a few k points to evaluate the Brillouin zone summation, since the magnetic properties depend on the Fermi surface. It is also supposed that we employ the spherical symmetric functions (39) as the localized function which generates the localized part of the mixed-basis set.

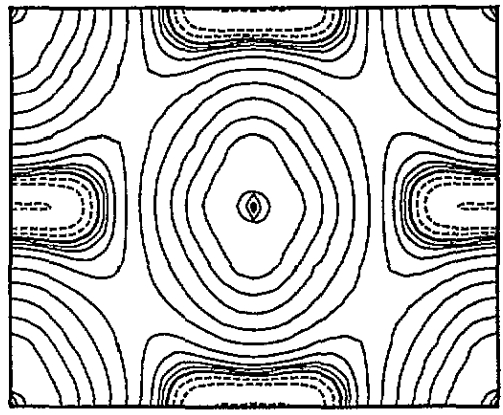

Figure 5. Contour of the spin density of iron on the (110) plane. The full contours represent the positive densities which start from $0.001e\,\mathrm{au}^{-3}$ to $0.256e\,\mathrm{au}^{-3}$ spacing by a factor of two in each contour. The broken contours are the negative densities which start from $-0.001e\,\mathrm{au}^{-3}$. The contours of zero density are drawn by thick curves.

The spin density on the (110) plane of the bulk iron is shown in figure 5. This figure clearly exhibits the anisotropy of the spatial distribution of the spin density. We also find that the areas of negative spin density appear in the interstitial region, originating from the spin polarization of the 4s electron. It is known [20] from measurement of the magnetic form factor by neutron diffraction that iron has these properties. The spin density evaluated here is consistent with experimental data.

6. Conclusions

We have presented a novel mixed-basis approach of *ab initio* molecular dynamics. In this approach, the mixed basis consists of plane waves and the Bloch function of localized functions connected to atoms in the unit cell. Localized functions that have analytic representations of the Fourier transform for the precise calculation are chosen. The functions in the mixed-basis set are orthonormalized with each other.

The equations of motion for the coefficients of expansion of the wavefunction by the mixed basis have been derived from the Car–Parrinello Lagrangian. These equations have a form that can be easily treated, because the derivatives of the coefficients are separated for each equation. All matrix elements of the Hamiltonian are represented by the Fourier components of the potentials and the localized part of the basis set. This representation has an advantage in calculation of the matrix elements using FFT. Because of the orthonormalization conditions for the basis set, the expressions of the matrix elements are simpler than the non-orthonormal basis. We have also obtained an explicit expression for the Pulay term of the force in this approach. This is due to the expressions of Fourier expansions for the localized part of the basis set.

We applied the mixed-basis approach to calculate the electronic structure and the lattice dynamics of diamond and iron. For diamond, properties such as the lattice constant, bulk modulus and phonon frequency are in good agreement with experimental data. We have demonstrated an efficient calculation for materials with spin polarization, in particular bcc iron. The lattice constant and the magnetic moment calculated here are comparable to those

measured in many experiments. In these calculations the mixed-basis approach leads to a decrease in memory usage in computers and in CPU time.

Acknowledgment

We are grateful to K Ando of the Toshiba Corporation for continuous encouragement.

References

[1] Car R and Parrinello M 1985 *Phys. Rev. Lett.* **55** 2471
[2] Hamann D R, Schlüter M and Chiang C 1979 *Phys. Rev. Lett.* **43** 1494
Bachelet G B, Hamann D R and Schlüter M 1982 *Phys. Rev.* B **26** 4199
[3] Vanderbilt D 1990 *Phys. Rev. Lett.* **41** 7892
[4] Laasonen K, Car R, Lee C and Vanderbilt D 1991 *Phys. Rev.* B **43** 6796
[5] Laasonen K, Pasquarello A, Car R, Lee C and Vanderbilt D 1993 *Phys. Rev.* B **47** 10142
[6] Louie S G, Ho K-M and Cohen M L 1979 *Phys. Rev.* B **19** 1774
[7] Kang M H, Tatar R C, Mele E J and Soven P 1987 *Phys. Rev.* B **35** 5457
[8] Elsässer C, Takeuchi N, Ho K-M, Chan C T, Braun C T and Fähnle M 1990 *J. Phys.: Condens. Matter* **2** 4371
Ho K-M, Elsässer C, Chan C T and Fähnle M 1992 *J. Phys.: Condens. Matter* **4** 5189
[9] Jansen R W and Sankey O F 1987 *Phys. Rev.* B **36** 6520
Jansen R W and Klein B M 1989 *J. Phys.: Condens. Matter* **1** 8359
[10] Rappe A M, Dal Pino A Jr, Needels M and Joannopoulos J D 1992 *Phys. Rev.* B **46** 7353
[11] Yin M T and Cohen M L 1981 *Phys. Rev.* B **24** 6121
[12] Hamann D R 1979 *Phys. Rev. Lett.* **42** 662
Bachelet G B, Greenside H S, Baraff G A and Schlüter M 1981 *Phys. Rev.* B **24** 4745
[13] Jones R O and Gunnarsson O 1989 *Rev. Mod. Phys.* **61** 689
[14] Srivastava G P and Weaire D 1987 *Adv. Phys.* **36** 463
[15] Hamann D R 1989 *Phys. Rev.* B **40** 2980
[16] Kleinman L and Bylander D M 1982 *Phys. Rev. Lett.* **48** 1425
[17] Perdew J P and Zunger A 1981 *Phys. Rev.* B **23** 5048
[18] Warren J L, Yarnell J L, Dolling G and Cowley R A 1967 *Phys. Rev.* **158** 805
Pavone P, Karch K, Schütt O, Windl W, Strauch D, Giannozzi P and Baroni S 1993 *Phys. Rev.* B **48** 3156
[19] Greenside H S and Schlüter M A 1983 *Phys. Rev.* B **27** 3111
[20] Shull C G and Mook H A 1966 *Phys. Rev. Lett.* **16** 184